Journal of Orthopaedic Translation 22 (2020) 2–6

Contents lists available at ScienceDirect

Journal of Orthopaedic Translation

journal homepage: www.journals.elsevier.com/journal-of-orthopaedic-translation

Perspectives

Facile fabrication of the zoledronate-incorporated coating on magnesium alloy for orthopaedic implants

Shanshan Chen [b], Peng Wan [c,***], Bingchun Zhang [b], Ke Yang [b,*], Yuhai Li [a,**]

[a] School of Material, Shenyang Ligong University, Shenyang 110168, China
[b] Institute of Metal Research, Chinese Academy of Sciences, Shenyang 110016, China
[c] School of Mechanical Engineering, Dongguan University of Technology, Dongguan 523808, China

ARTICLE INFO

Keywords:
Biodegradable
Drug loading
Magnesium alloy
Orthopaedic implant
Zoledronate

ABSTRACT

Background: Bisphosphonates (BPs) are known as a group of well-established drugs which are clinically used in metabolic bone disorder-related therapies. Recently increasing interests are focused on the application of BPs in the biodegradable Mg-based implants.
Methods: In this study a facile method was applied to fabricate a zoledronate loaded coating on AZ31 Mg alloy in comparison with the previous construction strategies, such as Ca-P chelation with BPs.
Results: The results showed that the fluoride pretreated coating could provide better corrosion resistance. Zoledronic acid (ZA) was successfully loaded on the surface of Mg alloy detected by X-ray photoelectron spectroscopy (XPS) and Fourier transform infrared (FTIR) analysis, and the release profile was quantified with Ultraviolet (UV) detection.
Conclusion: It is considered that this construction of ZA coated Mg-based orthopedic implants could be easily and efficiently used in clinic.
The translational potential of this article: Different from the traditional drug release mode, this paper used the hydrogen bond between drug molecules and drug carriers to not only realise the effective drug release in the early stage of drug release, but also meet the continuous effect of drugs in the later stage, providing a new possibility for clinical application.

Introduction

An ageing population and increasing bone-related disease are posing significant challenges in the coming decades. There is urgent demand for patient rehabilitation associated with the increase in life expectancy with the help of medical devices or fixtures. Current development of novel orthopaedic implants is aimed to accelerate the healing of large bone fractures and treat established nonunion problematic fractures [1]. In addition, with the rise of trauma victims and musculoskeletal disorders, therapeutic drugs in combination with implants or tissue-engineering approaches for bone regeneration are increasingly considered in clinical application [2,3].

Recently, the application of bisphosphonates (BPs) is attracting more and more interest, and the related studies are also growing with evidence of advantages of BPs [4–6]. BPs are well-established drugs that are used in the development of therapies for metabolic bone disorders, such as osteoporosis and Paget's disease, tumour-induced hypercalcaemia, and inflammation-related bone loss [7,8]. BPs not only inhibit bone resorption induced by osteoclasts but also accelerate bone formation induced by osteoblasts, which is in relation to the concentration of BPs [9–11].

In the past 30 years, the use of BPs is mainly connected with stainless steel or titanium alloy implants in clinical field, and their efficacy has been proved both *in vitro* and *in vivo* [12–14]. Compared with these conventional permanent metallic fracture fixations, magnesium (Mg) alloys have emerged as promising next-generation implants owing to their characteristic of degradation in the biological environment, which can avoid the second surgery for removal of the implant and incidental adverse effects or complications. Besides, the degradation of Mg alloy has also been verified to promote the bone formation [15].

The novel strategy by combination of BPs and Mg alloy implants has been proposed by some researchers based on different indications and

* Corresponding author. Institute of Metal Research, Chinese Academy of Sciences, 72 Wenhua Road, Shenyang 110016, China.
** Corresponding author. School of Material, Shenyang Ligong University, Shenyang 110168, China.
*** Corresponding author. School of Mechanical Engineering, Dongguan University of Technology, Dongguan 523808, China.
E-mail addresses: wanpeng@dgut.edu.cn (P. Wan), kyang@imr.ac.cn (K. Yang), yuhai_li@qq.com (Y. Li).

https://doi.org/10.1016/j.jot.2019.09.007
Received 24 March 2019; Received in revised form 20 September 2019; Accepted 22 September 2019
Available online 18 October 2019

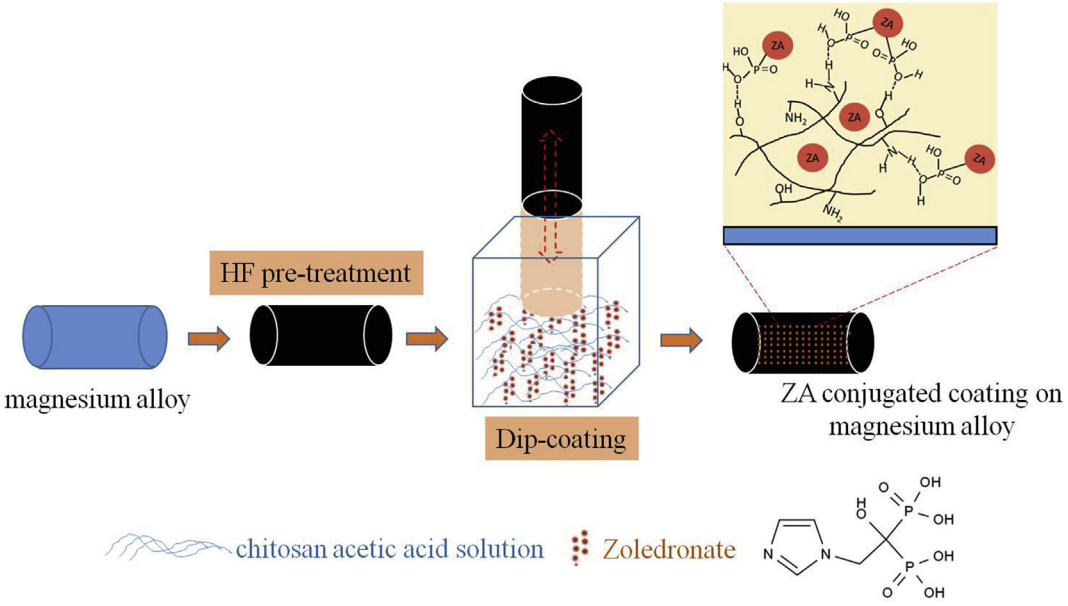

Fig. 1. Schematic picture of the coating fabrication process. HF = hydrofluoric acid; ZA = zoledronate.

hypotheses. Li et al. [16] reported a zoledronate (ZA)-loaded Mg–Nd–Zn–Zr alloy to improve osteoporotic fracture healing by dual modulation of bone formation and resorption. Similarly, Li et al. [17] studied the regulation of osteogenesis and osteoclastogenesis by loading zoledronic acid on a biodegradable Mg–Sr alloy. Molecular and cellular mechanisms for ZA-loaded Mg alloys to inhibit giant cell tumours of bone are discussed in a latest research study [18].

In this work, a facile method with combination of fluoride pretreatment and dip coating was applied in development of the ZA-loaded coating on AZ31 Mg alloy in comparison with previous construction

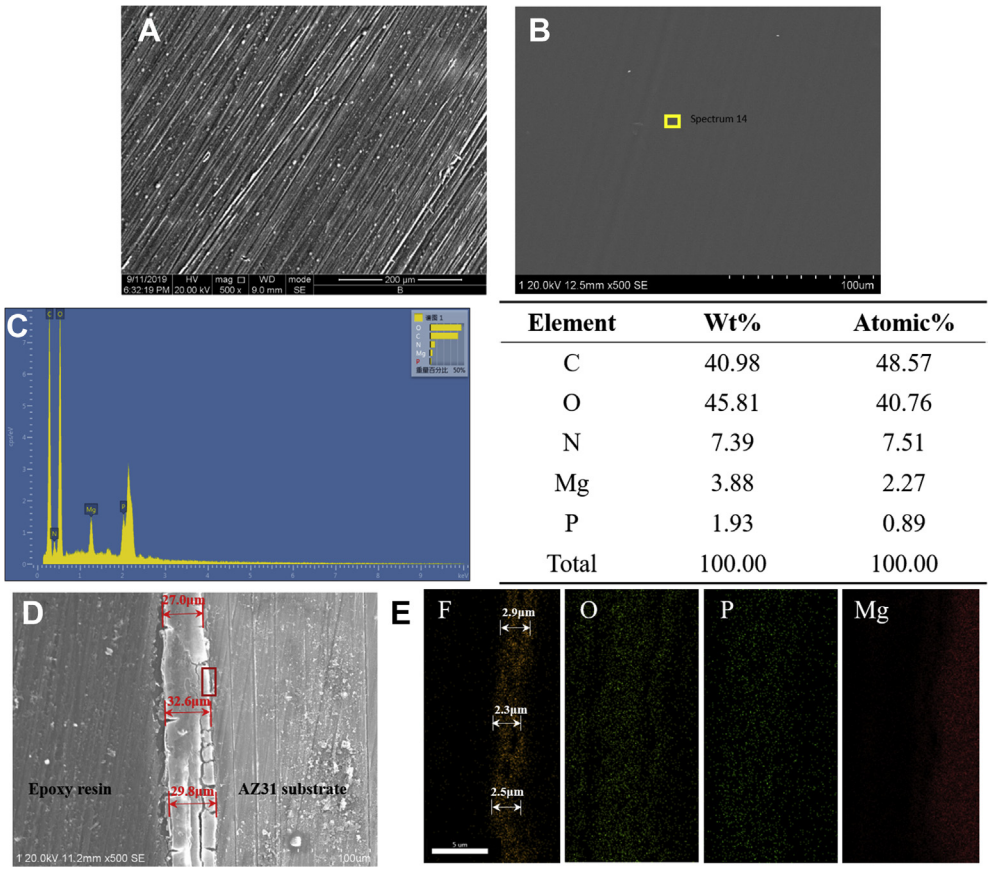

Element	Wt%	Atomic%
C	40.98	48.57
O	45.81	40.76
N	7.39	7.51
Mg	3.88	2.27
P	1.93	0.89
Total	100.00	100.00

Fig. 2. (A) Surface of the naked Mg alloy, (B) surface, (C) EDS point scan results, (D) cross-sectional morphologies, and (E) mapping scan results of the ZA-incorporated coating, obtained by scanning electron microscopy. EDS = energy-dispersive spectroscopy; ZA = zoledronate.

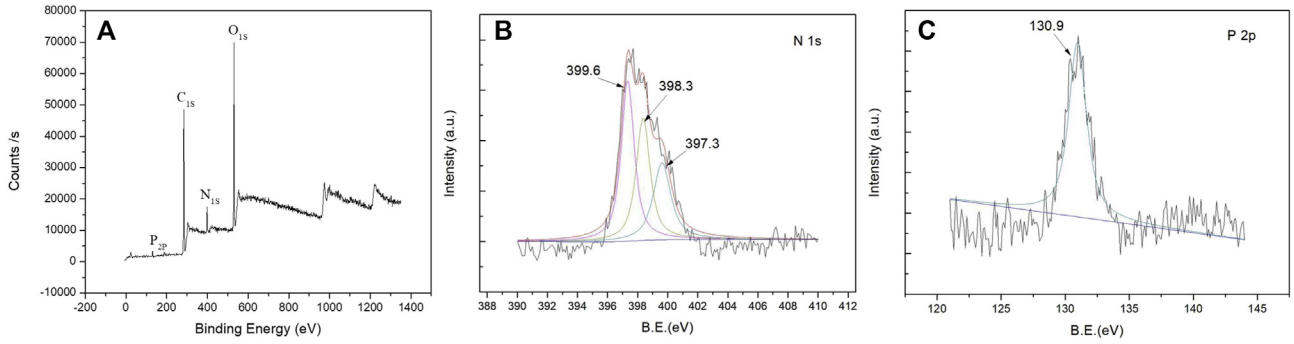

Fig. 3. (A) XPS survey spectra and high-resolution spectra of (B) nitrogen N 1s and (C) P 2p for the zoledronate-incorporated coating. XPS = X-ray photoelectron spectroscopy.

strategies, such as Ca–P chelation with BPs. In many previous studies, fluoride treatment was considered an effective method to improve the corrosion resistance [19–21]. Immobilised ZA on the pretreated fluoride coating was hypothesised to be associated with better corrosion resistance and valid drug release for AZ31 Mg alloy.

Materials and methods

Materials and coating preparation

An AZ31 Mg alloy (Mg–3% Al–1% Zn) was used as the substrate in this work, which was studied as the orthopaedic implant in the previous work [22]. AZ31 substrates were pretreated with hydrofluoric acid (HF) treatment for 24 h to form a fluoride coating according to our previous protocol [21]. ZA (10^{-4} mol/mL) was immersed in 3 mL of 1% chitosan acetic acid solution (concentration of acetic acid solution = 1%). The fluoride-coated AZ31 substrates were then immersed in the aqueous ZA solution five times by the dip coating method at room temperature and dried using a gentle stream of dry air. Because ZA is uniformly blended in the coating solution, ZA is evenly distributed in the coating as a blend. There is also a possibility of hydrogen bonding between the phosphate group in ZA and amidogen/oxhydryl group in chitosan. Based on this, the bonded ZA will keep long-term maintenance of efficacy. The schematic picture of the process is shown in Fig. 1.

In vitro degradation

Three samples with the ZA coating and naked AZ31 samples as the control were immersed in 5 mL of phosphate-buffered saline at 37 °C for 1, 4, 7, and 14 days to detect Mg^{2+} concentration. Meantime, pH variation of the solution was monitored during the immersion periods, and the corrosion rate of the substrate was calculated by weight loss after immersion for 14 days. The following is the calculation formula:

$$CR = \frac{(W_0 - W_t) \times 365}{\rho \times s \times t}$$

where W_0 is the initial weight of the sample before the immersion test, W_t is the weight of the sample after immersion for t days, ρ is the density of the substrate, s is the surface area of the sample, and t is the immersion time.

Surface description of the ZA-loaded coating

The morphologies and compositional profiles of the ZA-loaded coatings were examined under a scanning electron microscope (S–3400N; Hitachi, Japan) equipped with energy-dispersive spectroscopy. X-ray photoelectron spectroscopy (XPS) was used to investigate the ZA adsorption on the surface. Analysis of the samples was performed by XPS (PHI 5600; PerkinElmer, Physical Electronics, Japan) using an Mg *K*α radiation source at a power of 300 W. The detected elements were observed from the survey spectrum over a range of 0–1100 eV with an energy resolution of 1.5 eV. The XPS bonding energy (BE) values were charge corrected with respect to those of adventitious carbon at 284.8 eV. High-resolution XPS spectra were collected by an energy resolution of 0.75 eV for key elements identified from the survey spectra. Fourier-transform infrared spectroscopy (FTIR) with attenuated total reflectance was performed aiming at detecting any type of chemical modification on the chemical structure of samples. The acquisition was performed in the transmittance mode from 4000 to 400 cm^{-1}. All the spectra were recorded using 64 scans and 2 cm^{-1} resolution on an FTIR spectrophotometer (PerkinElmer 1600 Series, United States).

In vitro drug release of the ZA-loaded coating

The release of ZA from the coating and the total amount of ZA loaded on the coating were measured using the UV/Vis spectrophotometer (752N; INESA, China). Primary stock standard solutions of ZA (0.5 mg/mL) were prepared and then diluted with deionised water to obtain a series of working solutions (0, 5, 10, 50, 100, and 500 μg/mL). The concentration of ZA release in the medium was determined during different immersion periods using the UV/Vis spectrophotometer at a wavelength of 210 nm. The ZA-loaded samples were immersed in the acetic acid solution with 1% concentration under ultrasonic oscillation for 3 min. The total amount of ZA loaded was detected using the same method.

Results and discussion

Fig. 2 shows the morphology of the ZA-conjugated coatings formed on the surface of AZ31 alloy after treatment with ZA at 10^{-4} mol/L; the concentration was chosen according to the previous article [16]. As described in the previous article [19], the fluoride coating showed a dense, black, and smooth conversion film on the surface. After incorporating a low concentration of ZA, the surface of the sample became more smooth and uniform, as shown in Fig. 2B. As the control sample, there were more scratches on the surface of the naked Mg alloy sample formed by grinding, as presented in Fig. 2A. It revealed that the morphology of the coating was uniform and smooth. The composition of the coating is shown in Fig. 2C; C, O, N, Mg, and P were present. For showing the structure of the coating, a mapping scan was performed, and the results of the location of the element distribution marked by the red rectangle in Fig. 2D are shown in Fig. 2E. It showed that Mg element is distributed in the AZ31 substrate, and F element is distributed in the inner fluoride coating. In addition, O and P elements are distributed in the whole ZA coating. The fluoride coating can be clearly found from the cross-sectional mapping image, the thickness of which is 2–3 μm. The previous study showed that the HF-treated coating could provide effective protection from corrosion of Mg [21]. On the outside of the fluoride

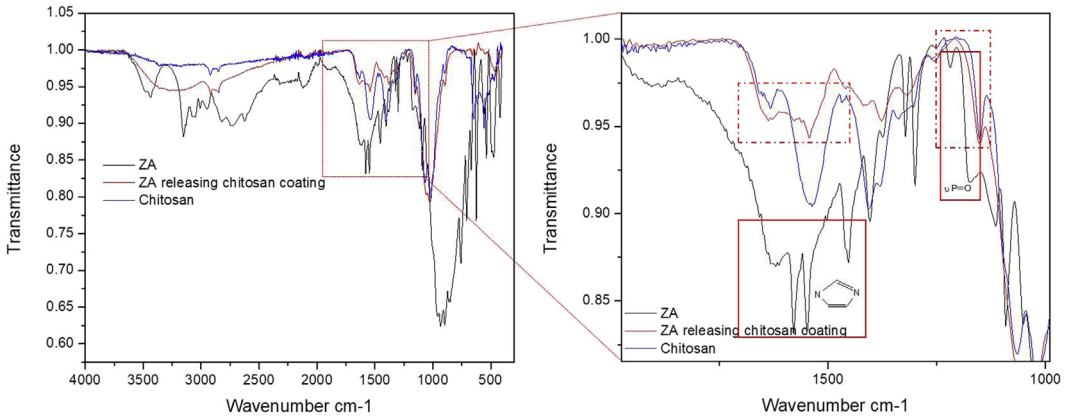

Fig. 4. FTIR-ATR spectra of ZA-incorporated coating. ZA powder was set as the reference. FTIR-ATR = Fourier-transform infrared spectroscopy with attenuated total reflectance; ZA = zoledronate.

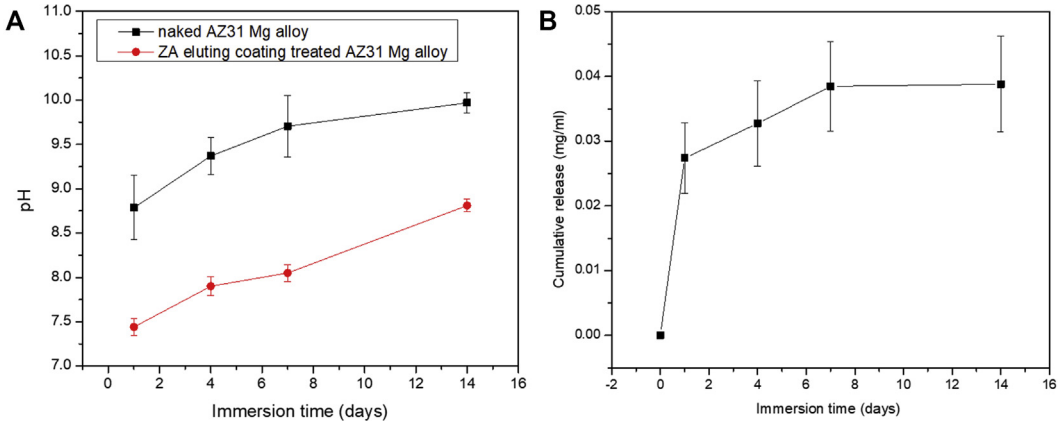

Fig. 5. (A) pH variation and (B) the zoledronate release profile during immersion periods of 14 days. ZA = zoledronate.

coating is the ZA coating, the average thickness of which is 29.8 ± 2.8 μm, as shown in Fig. 2D.

It is known that the BP structure consists of two oxidised phosphorous atoms linked by a central carbon (P–C–P). Besides, the side chains attached to the carbon are responsible for the property of BP. The R1 side chain substituted by the –OH group could increase BP's binding affinity. The R2 side chain determines the antiresorptive properties of the BP, and the nitrogen in an alkyl chain situated here increases the BP potency [23]. Thus, XPS was used for studying the adsorption of ZA, a commonly used nitrogenous BP [14]. The XPS survey spectrum of the ZA-incorporated coating is shown in Fig. 3. The N 1s and P 2p photoelectron signals are the markers of choice for confirming ZA adsorption. The N1s photoelectron signal was expected to be strong, and this is clearly evident in Fig. 3A. Comparatively, the XPS sensitivity factor for P 2p is relatively low. In addition to the N 1s and P 2p signals, the other observed photoelectron signals were carbon (284 eV) and oxygen (531.1 eV).

Fig. 3B shows the high-resolution N 1s spectrum for the ZA-incorporated coating. After curve fitting, the ZA coating showed three deconvoluted peaks at BEs of 399.6, 398.3, and 397.3 eV. This indicates that the N 1s signal detected by the survey spectrum scan was indeed due to the BP adsorption. The highest peak at a BE of 399.6 eV can be attributed to the presence of the NH_2 group in the BP. A similar result was reported by Yoshinari et al. [24] who detected a NH_2-like peak for pamidronate at 399.3 eV. Fig. 3C shows the P 2p peak detected at 130.9 eV, which is attributed to the possible phosphorous component in the BP. Yoshinari et al. [24] reported a slightly higher BE value at 133.8 eV for the PO_3^{2-} group in pamidronate.

Fig. 4 shows the FTIR spectra obtained for the ZA-incorporated coating. Compared with drug carrier polymer–chitosan, the presence of ZA could be detected and identified at characteristic bands of 1150 cm^{-1} ($\nu_{P=O}$), 1543–1635 cm^{-1} ($\nu_{C=N}$), and 1400 cm^{-1} ($\nu_{C=C}$) in the ZA-loaded coating according to a reference of pure ZA powder. In addition, the characteristic peak position of the free hydroxyl group and hydroxyl group in the phosphate group in ZA is at 3500 cm^{-1} and 2500–3300 cm^{-1}, respectively. After loading in the coating, the peak widened and intensity decreased, which indicated that the hydroxyl groups have bonded with chitosan to form an intermolecular hydrogen bond. It was verified that ZA had been loaded in the coating.

Fig. 5 indicates the pH variation and release of ZA from the coated AZ31 alloy. It can be found that the pH for the ZA-incorporated coating increased slowly from 7.4 to 8.8 over a period of 14 days. Compared with coated samples, the pH of the naked AZ31 alloy increased from 8.8 to 10.2 over a period of 14 days. The relatively low pH value is attributed to the excellent corrosion resistance of the fluoride coating, which has been proved in many studies [21,25]. According to the weight loss data, the corrosion rate after immersion for 14 days was calculated to be 4.8 × 10^{-4} mm/year. The release profile of the coating was measured by UV/Vis detection. The calibration curve was linear in the range of 5–500 μg/mL ($R^2 > 0.999$). The release of ZA was greatest during the first 7 days (0.04 mg/mL) and decreased rapidly during the next 7 days to reach a plateau. The initial burst release and sustainable release of ZA were

mainly attributed to the drug adsorption on the surface and insusceptible to the degradation of Mg alloy. In addition, the total amount of ZA loaded was also detected, which was 0.07–0.08 mg/mL. It was indicated that the release rate of ZA during the first 7 days was 50–60%. It can be inferred that nearly half of the drugs were hydrogen bonded to chitosan in the coating after 14 days of immersion.

Conclusion

To develop a novel drug-loading orthopaedic implant, we constructed an AZ31 Mg alloy coated with the anticatabolic ZA. It is believed that this design could improve bone formation and simultaneously inhibit excessive resorption owing to the degradation of Mg alloy. A facile method was applied by combination of fluoride pretreatment and the dip coating method in the ZA and chitosan–acetic acid mixed solution. The pH variation curve and corrosion rate calculated by weight loss exhibited excellent corrosion resistance of Mg alloy owing to a thick fluoride-pretreated coating. Zoledronic acid was successfully loaded on the surface of Mg alloy detected by X-ray photoelectron spectroscopy (XPS) and Fourier transform infrared (FTIR) analysis, and the release profile was quantified with Ultraviolet (UV) detection, which showed an initial appropriate burst release and sustainable release over a period of 14 days and retains some functional groups by the bonding formed. It is considered that this construction of ZA-coated Mg-based orthopaedic implants could be easily and efficiently used in the clinic.

Conflict of interest

The authors have no conflicts of interest to disclose in relation to this article.

Acknowledgements

This work was financially supported by an open fund of characteristic training discipline of Shenyang Ligong University (0101311008502), Youth Innovation Promotion Association, Chinese Academy of Sciences (no. 2019194), and the doctoral scientific research fund of Dongguan University of Technology (GC300501-082).

References

[1] Wozney JM, Seeherman HJ. Protein-based tissue engineering in bone and cartilage repair. Curr Opin Biotechnol 2004;15:392.
[2] Laurencin C, Ambrosio A, Borden M, Cooper J. Tissue engineering: orthopedic applications. Annu Rev Biomed Eng 1999;1:19.
[3] Mourino V, Boccaccini A. Bone tissue engineering therapeutics: controlled drug delivery in three-dimensional scaffolds. J R Soc Interface 2010;7:209.
[4] Farrell Kristen B, Karpeisky Alexander, Thamm Douglas H, Zinnen Shawn. Bisphosphonate conjugation for bone specific drug targeting. Bone Rep 2018;9:47–60.
[5] Mendes V, dos Santos GO, Calasans-Maia MD, Granjeiro JM, Moraschini V. Impact of bisphosphonate therapy on dental implant outcomes: an overview of systematic review evidence. Int J Oral Maxillofac Surg 2019;48(3):373–81.
[6] Young Robert N, Grynpas Marc D. Targeting therapeutics to bone by conjugation with bisphosphonates. Curr Opin Pharmacol 2018;40:87–94.
[7] Rodan G. Mechanism of action of bisphosphonates. Annu Rev Pharmacol Toxicol 1998;38:375.
[8] Shi X, Wang Y, Ren L, Gong Y, Wang D. Enhancing alendronate release from a novel PLGA/hydroxyapatite microspheric system for bone repairing applications. Pharm Res 2009;26:422.
[9] Reinholz G, Getz B, Pederson L, Sanders E, Subramaniam M, Ingle J, et al. Bisphosphonates directly regulate cell proliferation, differentiation, and gene expression in human osteoblasts. Cancer Res 2000;60:6001.
[10] Sahni M, Guenther H, Fleisch H, Collin P, Martin T. Bisphosphonates act on rat bone resorption through the mediation of osteoblasts. J Clin Investig 1993;91:2004.
[11] Vitte C, Fleisch H, Guenther H. Bisphosphonates induce osteoblasts to secret an inhibitor of osteoclast-mediated resorption. Endocrinology 1996;137:2324.
[12] Oliveira AL, Pedro AJ, Saiz Arroyo C, Mano JF, Rodriguez G, San Roman J, et al. Biomimetic Ca-P coatings incorporating bisphosphonates produced on starch-based degradable biomaterials. J Biomed Mater Res B Appl Biomater 2010;92B:55–67.
[13] Sahni Malika, Guenther Harald L, Fleisch Herbert, Pascal Collin, John Martin T. Bisphosphonates act on rat bone resorption through the mediation of osteoblasts. J Clin Investig 1993;91:2004–11.
[14] Cattalini Juan Pablo, Boccaccini Aldo R, Lucangioli Silvia, Mourino Viviana. Bisphosphonate-based strategies for bone tissue engineering and orthopedic implants. Tissue Eng A B 2012;18(5):323–40.
[15] Zhang Yifeng, Xu Jiankun, Ruan Ye Chun, Yu Mei Kuen, O'Laughlin Micheal, Wise Helen, et al. Implant-derived magnesium induces local neuronal production of CGRP to improve bone-fracture healing in rats. Nat Med 2016;22:1160–9.
[16] Li Guoyuan, Zhang Lei, Wang Lei, Yuan Guangyin, Dai Kerong, Jia Pei, et al. Dual modulation of bone formation and resorption with zoledronic acidloadedbiodegradable magnesium alloy implants improves osteoporotic fracture healing: an in vitro and in vivo study. Acta Biomater 2018;65:486–500.
[17] Li Mei, Wan Peng, Wang Weidan, Yang Ke, Zhang Yu, Han Yong. Regulation of osteogenesis and osteoclastogenesis by zoledronic acid loaded on biodegradable magnesium-strontium alloy. Sci Rep 2019;9:933.
[18] Li Mei, Wang Weidan, Zhu Ye, Lu Yao, Wan Peng, Yang Ke, et al. Molecular and cellular mechanisms for zoledronic acid-loaded magnesium-strontium alloys to inhibit giant cell tumors of bone. Acta Biomater 2018;77:365–79.
[19] Panemangalore Devadas Bhat, Shabadi Rajashekhara, Gupta Manoj, Ji Gang. Effect of fluoride coatings on the corrosion behavior of Mg–Zn–Er alloys. Surfaces Interfaces 2019;14:72–81.
[20] Fintová Stanislava, Drábiková Juliána, Pastorek Filip, Tkacz Jakub, Ptáček Petr. Improvement of electrochemical corrosion characteristics of AZ61 magnesium alloy with unconventional fluoride conversion coatings. Surf Coat Technol 2019;357:638–50.
[21] Yan Tingting, Tan Lili, Zhang Bingchun, Yang Ke. Fluoride conversion coating on biodegradable AZ31B magnesium alloy. J Mater Sci Technol 2014;30(7):666–74.
[22] Chen Shanshan, Zhang Bin, Zhang Bingchun, Lin Hao, Yang Hui, Zheng Feng, et al. Assessment of structure integrity, corrosion behavior and microstructure change of AZ31B stent in porcin. J Mater Sci Technol 2 Jan 2019. https://doi.org/10.1016/j.jmst.2018.12.017.
[23] Van Beek E, Lowik C, Que I, Papapoulos S. Dissociation of binding and antiresorptive properties of hydroxybisphosphonates by substitution of the hydroxyl with an amino group. J Bone Miner Res 1996;11:1492.
[24] Yoshinari M, Oda Y, Ueki H, Yokose S. Immobilization of bisphosphonates on surface modified titanium. Biomaterials 2001;22:709–15.
[25] Yan Tingting, Tan Lili, Xiong Dangsheng, Liu Xinjie, Zhang Bingchun, Yang Ke. Fluoride treatment and in vitro corrosion behavior of an AZ31B magnesium alloy. Mater Sci Eng C 2010;30(5):740–8.